Vanishing of the negative anode sheath in a Hall thruster

E. Ahedo[a] and J. Rus
Escuela Técnica Superior de Ingenieros Aeronáuticos, Universidad Politécnica de Madrid, 28040 Madrid, Spain

(Received 21 February 2005; accepted 18 July 2005; published online 23 August 2005)

The transition on a Hall thruster discharge from negative to zero anode sheaths is studied with a macroscopic, stationary model. Since electron drift velocities become of the order of the thermal velocity, inertial effects on electrons must be included in the model. For thrusters with the Hall parameter still large at the anode, these effects appear only in a thin region and bound the electron azimuthal velocity at the anode to values of the order of the thermal velocity. The no-sheath regime is reached when the discharge voltage is decreased and corresponds to a small and nonmonotonic portion of the voltage-current curve. Possible connections of this behavior with experimental results are suggested. Modifications on the discharge characteristics at the regime transition are analyzed. Energy losses at the lateral walls decrease with the discharge voltage, due to the changes on the temperature profile, whereas energy losses at the anode increase only moderately. The thrust efficiency presents a maximum within the negative-sheath regime. © *2005 American Institute of Physics*. [DOI: 10.1063/1.2032615]

I. INTRODUCTION

The near-anode region of a Hall thruster discharge is incompletely understood yet. Experiments and models have centered the research on the ionization and acceleration regions, which, in principle, are more relevant for the thruster response. The difficulties of carrying out direct plasma measurements of the channel rear region have hindered its analysis too. Nonetheless, the electron transport to the anode and the formation of a space-charge sheath at the anode are affecting the thruster operation. Zhurin *et al.*,[1] who reviewed the large Russian experience on Hall thrusters, assert that, under normal operation, electron thermal transport is more than sufficient to sustain the discharge and thus a negative sheath needs to be formed. When the thermal flux is insufficient to conduct the discharge current a positive sheath develops; Zhurin *et al.* associate this situation to too low propellant flows and indicate that it results in the discharge easily becoming extinguished.

Since a negative sheath is ion attracting, an indirect test of the presence of a negative sheath (or, more correctly, of the absence of a positive sheath) is ion backstreaming in the anode vicinity. Ion backstreaming (occupying up to a 60% of the channel length) was reported experimentally by Bishaev and Kim[2] and Kim.[3] Direct observations of the anode-sheath fall have been made recently by Dorf *et al.*[4] Positive and negative anode falls are found, depending on the anode being clean or coated by a dielectric and the values of the control parameters (discharge voltage V_d, mass flow, etc.). For clean anodes, potential falls were negative preferentially and the fall tended to decrease when V_d decreased.

The ion backstreaming region and the negative sheath are recovered in the discharge models of Fife,[5] Ahedo and Martínez-Sánchez,[6] Ahedo *et al.*,[7–9] and Barral *et al.*[10] All these models show that the anode fall decreases when V_d *decreases*, in agreement with the observations of Dorf *et al.* Furthermore, these models yield that the negative sheath vanishes for a "low" value of V_d, but Ahedo *et al.*[8] pointed out that electron inertial becomes relevant before the negative sheath vanishes, thus affecting the consistency of the diffusive model used for electrons. Dorf *et al.* have studied theoretically the transition to a no-sheath regime in two papers.[11,12] Contrary to the models cited previously, they found that the negative anode fall decreases as V_d *increases*. A key aspect of their models is to consider the temperature profile as an *input* of the model and *invariant* with V_d, instead of solving consistently the electron energy equation with the rest of plasma equations.

The present paper extends the negative-sheath model of Ahedo *et al.*[9] to a no-sheath regime based on the anode conditions proposed by Dorf *et al.* in Ref. 11. The contributions are (i) the computation of the temperature profile with the rest of plasma variables and (ii) the inclusion of electron inertia. We thus aim to present a more complete model of the discharge, to analyze the evolution of the discharge characteristics when transiting to the no-sheath regime, and to show that the discrepancy with the models of Dorf *et al.* on the evolution of the anode fall with V_d is caused mainly by the different treatment of the electron temperature. However, the comparison with these models will not be perfect since the Hall parameter in the channel rear region is small in their cases and large in ours.

II. REVIEW OF THE NEAR-ANODE REGION

A. The negative-sheath regime

A central feature for the proper operation of a Hall thruster is that the Hall parameter be large, i.e.,

$$\omega_e/\nu_e \gg 1, \tag{1}$$

with $\omega_e(=eB/m_e)$ the electron gyrofrequency and ν_e the total collision frequency (which, in general, includes contributions

[a]Electronic mail: eduardo.ahedo@upm.es

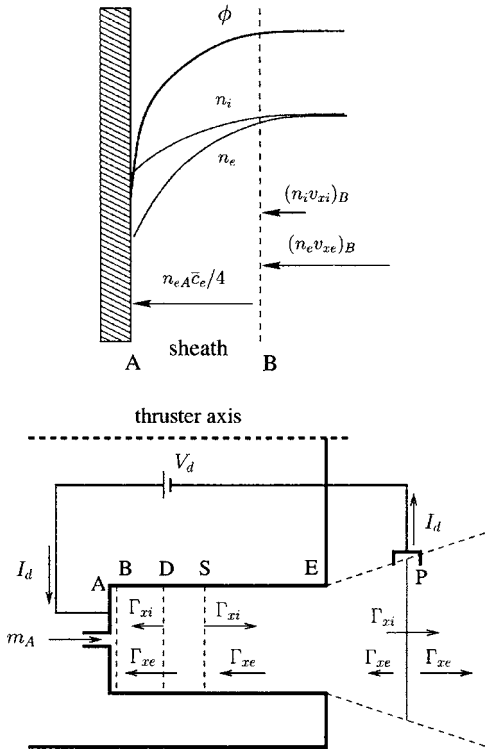

FIG. 1. (Top) The anode sheath. (Bottom) Sketch of the whole discharge model. The anode is at point A (with $x_A=0$), the thruster exhaust at point E, and the cathode neutralization surface at point P. Points D and S correspond to zero and sonic velocities of the ion flow and are part of the solution. Point B is the anode-sheath transition. Regions AB, BD, DS, and SP correspond to anode sheath, ion backstreaming region, main ionization layer, and acceleration region. $\Gamma_{x\alpha}=An_\alpha v_{x\alpha}$, $\alpha=i,e,\ldots$, are axial flows of particles of each of the plasma species.

from collisions with neutrals and with ions, wall collisionality, and Bohm diffusion). In addition and mainly as a consequence of condition (1), the electron motion along the chamber satisfies generally the collisional-diffusive condition

$$|v_e| \ll \bar{c}_e = \sqrt{8T_e/\pi m_e}, \tag{2}$$

with v_e the macroscopic velocity of electrons. Conditions (1) and (2) lead to a quasiclosed drift of the electrons, with the ratio between azimuthal (θ) and axial (x) velocities satisfying

$$v_{\theta e}/v_{xe} \simeq -\omega_e/\nu_e. \tag{3}$$

For an annular thruster channel and a metallic (clean) anode covering the rear wall, a negative sheath (Fig. 1) self-adjusts the electron thermal current collected by the anode to the small diffusive current of electrons at the channel rear region. Assuming a quasi-Maxwellian distribution function, the potential drop in the sheath, $\phi_{AB}=\phi_B-\phi_A$, comes out from

$$\frac{\bar{c}_{eB}}{4}\exp\frac{-e\phi_{AB}}{T_{eB}} = -v_{xeB} \tag{4}$$

(notice that $v_{xe}<0$). The electric field in the quasineutral region next to the anode sheath has the same sign than the electric field inside the sheath and accelerates the ion flow towards the anode. Therefore, the existence of a negative sheath implies the formation of an ion backstreaming region (BD in Fig. 1) in the quasineutral discharge. As it is well known, the sheath/plasma transition is defined by the Bohm sonic condition for the velocity of the attracted species (i.e., ions); for $T_i \ll T_e$ the Bohm condition reads

$$v_{xiB} = -\sqrt{T_{eB}/m_i}, \tag{5}$$

with v_{xi} the axial macroscopic velocity of ions. Equations (4) and (5) yield that the sheath potential drop depends directly on the ion backstreaming current:

$$\frac{e\phi_{AB}}{T_{eB}} = \ln\left(\sqrt{\frac{m_i}{2\pi m_e}}\frac{|I_{iB}|}{I_d+|I_{iB}|}\right). \tag{6}$$

Here, $I_d[=I_i(x)-I_e(x)]$ is the discharge current, I_α $[=en_e v_{x\alpha}A_c$ $(\alpha=i$ and $e)]$ is the current of species α (with I_e negative and I_i changing sign at point D), and A_c is the area of the channel cross section. For good thruster operation one expects I_{iB}/I_d to be small (less than, say, 10%), so that $|I_{eB}|\simeq I_d$.

B. The no-sheath regime and inertial effects

From the above equations, the sheath vanishes when

$$\frac{|I_{iB}|}{I_d} \simeq \sqrt{\frac{2\pi m_e}{m_i}}, \tag{7}$$

(for xenon, this means $-I_{iB}/I_d \simeq 0.5\%$) and the electron drifts at the anode satisfy

$$v_{xeB} = -\frac{\bar{c}_{eB}}{4} = -\sqrt{\frac{T_{eB}}{2\pi m_e}}, \tag{8}$$

$$v_{\theta eB} \simeq -\frac{\omega_{eB}}{\nu_{eB}}v_{xeB}. \tag{9}$$

In terms of the parameters governing the discharge, Ahedo *et al.* found that $-I_{iB}/I_d$ decreases when either V_d decreases or the strength of the radial magnetic field $B_{\max}$ increases (see Figs. 5 and 7 of Ref. 7 and Fig. 6 of Ref. 8). The works of Barral *et al.*[10] and Cohen-Zur *et al.*[13] also conclude that the no-sheath regime is reached when the discharge voltage is decreased. (The particular value of V_d for the no-sheath limit depends on $B_{\max}$ and other thruster parameters.)

Reference 8 (see Sec. 4 B) showed that the collisional-diffusive hypothesis could fail near the anode already within the negative-sheath regime. The specific situation depends on the value of the Hall parameter near the anode, which depends on the design of the magnetic-field profile in the rear part of the channel. A simple look at the literature on Hall thrusters identifies three typical situations:

(1) Equation (1) is satisfied up to the anode, so that electrons are magnetized in the whole channel. For this case, Eqs. (8) and (9) show that condition (2) fails when the no-sheath limit is approached. Therefore, electron inertia needs to be included in order to treat consistently the rear region in the no-sheath regime.
(2) Equation (1) is satisfied except around an internal point where the magnetic field changes sign. Then, electron inertia is relevant also around the point where the magnetic field crosses zero and $v_{\theta e}$ changes rather abruptly.
(3) The magnetic field is negligible and ω/ν_e becomes small

in the channel rear region. Then, *independently* of the anode fall, the electron motion in the rear region is governed mainly by inertia. If the resistivity is small, electrons keep the azimuthal velocity acquired in the front region of the channel.

In Ref. 11, Dorf *et al.* analyze the transition to a no-sheath regime with a macroscopic model for electrons. The no-sheath regime is characterized by substituting condition (5) by condition (8) and $\phi_{AB}=0$. The ion velocity at the anode should be subsonic, $-\sqrt{T_{eB}/m_i}<v_{xiB}<0$. (For convenience, we keep naming point B to the anode boundary of the quasineutral model, even when it coincides with point A). Dorf *et al.* apply their model to cases with ω/ν_e small in the rear region but they still use the diffusive electron model in the whole channel. In Ref. 12 they try to solve this inconsistency by using different electron models in the front and rear regions of the channel. As commented before, in both papers of Dorf *et al.*, consider the temperature profile as an input function and invariant with V_d.

III. A MODEL WITH INERTIAL EFFECTS ON ELECTRONS

Here, we study the transition to the no-sheath regime with the macroscopic formulation of Ref. 9 and applying the shift of anode conditions [from Eq. (5) to Eq. (8)] proposed in Ref. 11. We consider thrusters satisfying Eq. (1) in the whole channel, so that the inertial effects are partial and affect only a thin region close to the anode.

When $v_{\theta e}\gg|v_{xe}|$, Ahedo *et al.*[8] showed that electron inertia counts first in the azimuthal momentum equation and proposed the following momentum equations:

$$0=-\frac{d(n_eT_e)}{dx}+en_e\frac{d\phi}{dx}+m_e\omega_e n_e v_{\theta e}, \tag{10}$$

$$v_{xe}\frac{dv_{\theta e}}{dx}=-v_{xe}\omega_e-\nu_e v_{\theta e}, \tag{11}$$

which has been used too by Barral *et al.*[10] The diffusive limit corresponds to take zero in the left-hand side of the last equation. Following Ref. 9, these two equations are completed with seven more, which determine the nine plasma variables of the discharge: n_e, v_{xe}, $v_{\theta e}$, v_{xi}, n_n, v_{xn}, ϕ, the electron temperature T_e, and the axial heat conduction q_{xe}.

A correct numerical integration of Eq. (11) requires to proceed along the direction of the electron motion, that is, from the neutralizer surface P to the anode sheath B (Fig. 1). However, this is not feasible in practice for the set of nine equations, due to other numerical constraints. In particular, it is known from the integration of the diffusive model in Ref. 8 that solutions launched from point S towards B have extreme difficulties in fulfilling the condition at B for the heat conduction q_{xe}. Indeed, the practical procedure was to launch two solutions from B and S, respectively, and match them at an intermediate point. (Then, a third solution is launched from S towards P to complete the integration.)

The above numerical constraints forced us to use an approximate scheme to solve the present case. This consists on the following: First, to substitute Eq. (11) by an approximate equation, which can be integrated with the rest of plasma equations using the above three-parts integration scheme. Let $v'_{\theta e}$ be the approximation of the azimuthal velocity obtained in this way. Second, Eq. (11) is solved in a postprocess to obtain $v_{\theta e}(x)$. The comparison of the two velocities $v'_{\theta e}$ and $v_{\theta e}$ evaluates the correctness of the procedure.

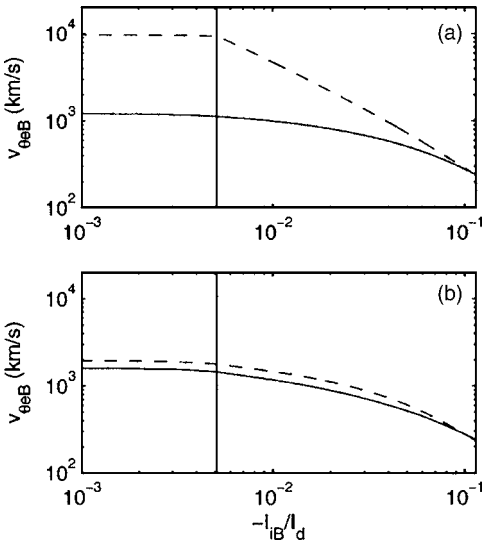

FIG. 2. Comparison between approximate (dashed) and correct (solid) solutions of $v_{\theta eB}$ for the (a) diffusive and (b) the inertia/diffusive models [Eqs. (12) and (13)], respectively. The vertical line marks the no-sheath limit. Thruster parameters correspond to an SPT-100 and are similar to those used in case 2 of Ref. 9.

Two different models for the approximate velocity $v'_{\theta e}$ have been tested. The first one is just the diffusive model,

$$v'_{\theta e}=-v_{xe}\omega_e/\nu_e. \tag{12}$$

The second one is a mixed inertial/diffusive one, where inertial effects are assumed to matter only in the near-anode region:

$$v'_{\theta e}=\begin{cases} v'_{\theta e,0}+v'_{\theta e,1}, & \text{for } x<x_t,\\ -v_{xe}\omega_e/\nu_e, & \text{for } x>x_t, \end{cases} \tag{13}$$

with $v'_{\theta e,0}$ and $v'_{\theta e,1}$ the solutions of

$$dv'_{\theta e,0}/dx=-\omega_e, \tag{14}$$

$$dv'_{\theta e,1}/dx=-v'_{\theta e,0}\nu_e/v_{xe}, \tag{15}$$

and x_t a convenient point to match the two types of solutions in Eq. (13).

Since I_{iB}/I_d is the convenient parameter to study the regime transition of the anode sheath, we take it as an input parameter instead of the discharge voltage V_d. All the results presented in the paper are for a thruster configuration close to case 2 of Ref. 9 (and similar to an SPT-100ML).

For both models of $v'_{\theta e}$, differences between $v'_{\theta e}(x)$ and $v_{\theta e}(x)$ are largest at the sheath transition, point B. Figures 2(a) and 2(b) compare $v'_{\theta eB}$ and $v_{\theta eB}$ for both models. For the diffusive approximation [Fig. 2(a)] the differences become significant for $-I_{iB}/I_d<5\%$ and are about 900% at the no-sheath regime ($-I_{iB}/I_d\leqslant 0.5\%$). The inertia/diffusive ap-

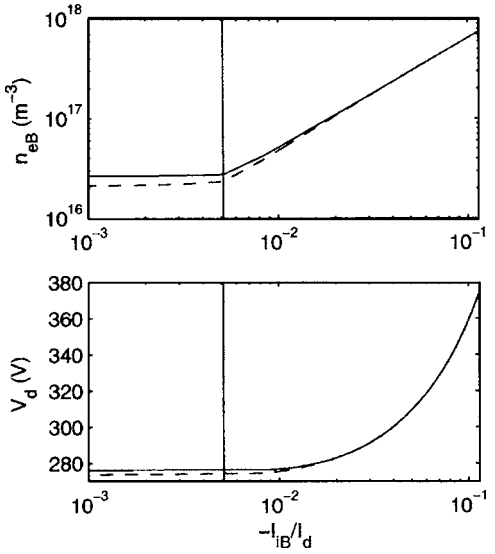

FIG. 3. Discharge voltage and plasma density at the anode-sheath transition when the diffusive (dashed) and the inertia/diffusive (solid) models for $v_{\theta e}$ are used. The vertical line marks the no-sheath limit. The rest of the parameters as in Fig. 2.

proximation [Fig. 2(b)] yields much better results: differences at the no-sheath regime are only about 20%.

Figure 3 compares the evolution of V_d and n_{eB} with I_{iB}/I_d for the two approximate models of the azimuthal velocity. In spite that Eq. (12) is overestimating the azimuthal velocity (and the axial magnetic force) at the anode up to one order of magnitude, this does not produce significant errors on the rest of the plasma variables, including on $v_{\theta e}$ when this is postcomputed. Thus, we can say that the mixed inertial/diffusive model is preferable to compute the main set plasma variables, and, in any case, the azimuthal velocity profile must always be computed from solving independently Eq. (11). A correct value of $v_{\theta e}$ is crucial, for instance, to evaluate the electron energy deposited at the anode, which is equal to

$$P_{\text{anode},e} = A_c (n_e v_{xe})_B \left[2T_e + \frac{m_e}{2}(v_{\theta e}^2 + v_{xe}^2) \right]_B . \tag{16}$$

The reason that inertial effects, although of dominant order in the no-sheath regime, have a limited effect on the plasma response is that they are very localized around the anode. This is true only when the Hall parameter is large in the whole channel. For $\omega_e/\nu_e < 1$ in a large region, the approximate treatment proposed here is not correct (and does not converge well): inertial effects are not local, they affect v_{xe} too, and are not limited to the no-sheath regime.

IV. PERFORMANCE ANALYSIS OF THE TWO ANODE REGIMES

Figure 4 compares the evolution of the main plasma parameters in the anode-sheath and no-sheath regimes. The inertial/diffusive model for $v'_{\theta c}$ has been used in the computations. Although I_{iB} is plotted as the abscissa, the real control parameter would be V_d. The rest of control parameters remain unchanged, in particular, the magnetic field strength is constant ($B_{\max} \simeq 230$ G). Figures 5 and 6 show axial profiles of the main plasma variables for three particular cases of Fig. 4: an intermediate negative-sheath point, the no-sheath limit, and the zero ion backstreaming limit.

The first result that stands out from Fig. 4 is that the no-sheath regime is reached when V_d is decreased. Second, this regime corresponds to a practically constant value of V_d, which means that it is bad defined in terms of the discharge voltage. Third, the parametric interval for the no-sheath re-

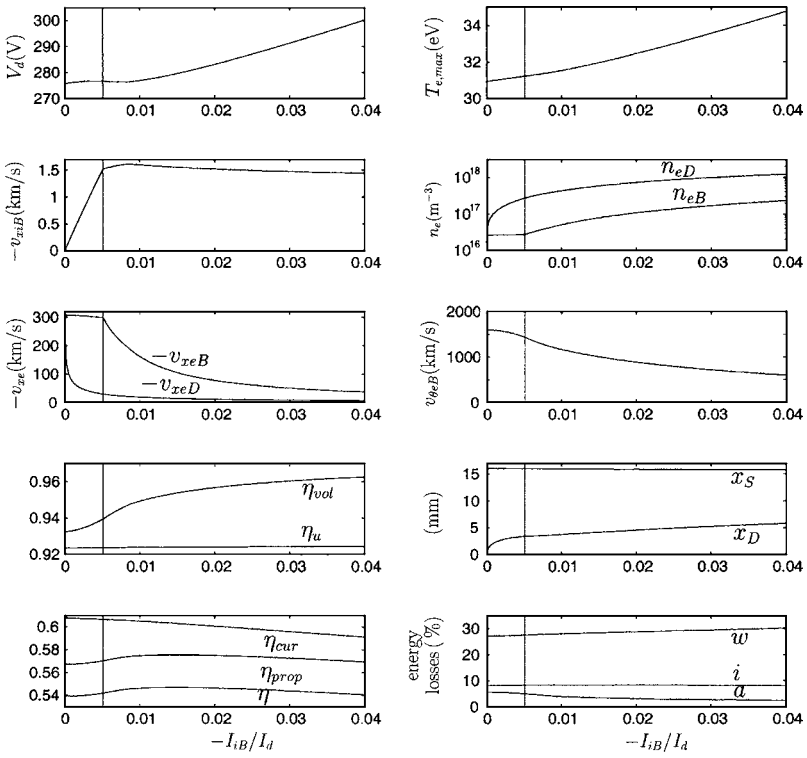

FIG. 4. Evolution of the main plasma parameters with the ion-reverse current at the anode. The rest of the parameters as in Fig. 2. The vertical line marks the no-sheath limit. In the last plot, w, i, and a refer to lateral wall, ionization, and anode losses, respectively.

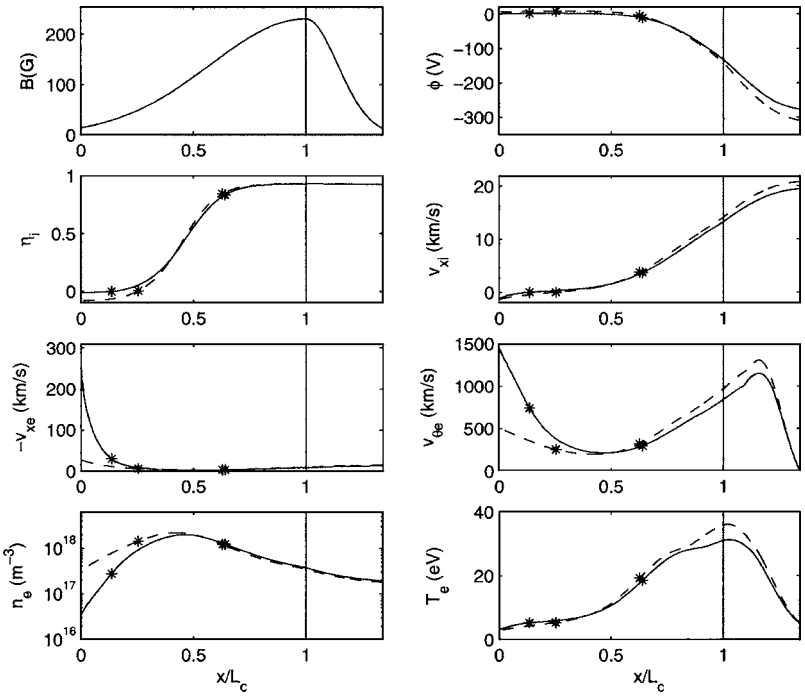

FIG. 5. Negative-sheath regime. The axial profiles of plasma variables for $-I_{iB}/I_d=5\times10^{-2}$ (dashed lines) and 5×10^{-3} (solid lines; no-sheath limit). The vertical line marks the channel exit. The asterisks represent points D (left) and S (right). The rest of the parameters as in Fig. 2.

gime is very narrow and changes on the axial profiles (Fig. 6) are null except in a small region near the anode.

The temperature profile and, in particular, its peak value $T_{e,\max}$ do not remain constant as the discharge voltage changes. The variation of the peak electron temperature with V_d is due to the electron Joule heating in the acceleration regime. The plots show that the temperature variations are relatively large,

$$\frac{\partial \ln T_{e,\max}}{\partial \ln V_d} > 2,$$

for most of the negative-sheath regime. This variation of the temperature profile agrees well with the experimental observations of Raitses *et al.*[14] and we believe is the main cause explaining the different response of the anode fall with V_d, with respect to Ref. 11.

The plasma density and velocities at point B change from satisfying

$$v_{xiB} \sim \text{const}, \quad n_{eB} \propto |I_{iB}|, \quad v_{xeB} \propto |I_{iB}|^{-1}, \tag{17}$$

for the negative-sheath regime, to fulfill

$$v_{xiB} \propto |I_{iB}|, \quad v_{xeB} \sim \text{const}, \quad n_{eB} \sim \text{const}, \tag{18}$$

for the no-sheath regime. The mild changes on v_{xiB} and of v_{xeB} within the negative-and no-sheath regimes, respectively, are due to T_{eB}, which lies between 3 and 5 eV. Notice the low values of n_{eB} in the no-sheath regime.

As I_{iB} decreases, point S remains almost invariant and point D (of zero ion velocity) drifts towards the anode. Thus, the acceleration region is not modified but the (main) ionization region (bounded approximately by points D and S) extends towards the anode. The extended ionization region permits the plasma density to be very low at B while keeping similar maximum values near point S. At the same time, it explains the decrease of the voltage efficiency $\eta_{\text{vol}}=\dot{m}_{i\infty}v_{xi\infty}^2/2eV_d$, which is responsible of the decrements of the propulsive and thrust efficiencies $[\eta_{\text{prop}}(I_{iB})\equiv P_{\text{use}}/P_d$ and $\eta\equiv F^2/2\dot{m}_A P_d \simeq \eta_u\eta_{\text{prop}}$, respectively] in the no-sheath and low-V_d range of the negative-sheath regimes; $\eta_{\text{cur}}=I_{i\infty}/I_d$ is the current efficiency and verifies $\eta_{\text{cur}}\simeq\eta_{\text{prop}}/\eta_{\text{vol}}$.[15] The propellant utilization $\eta_u=\dot{m}_{i\infty}/\dot{m}_A$, which depends on the balance between ionization and wall recombination on the acceleration region,[9] remains almost constant with I_{iB}.

The effects of electron inertia are very evident in the

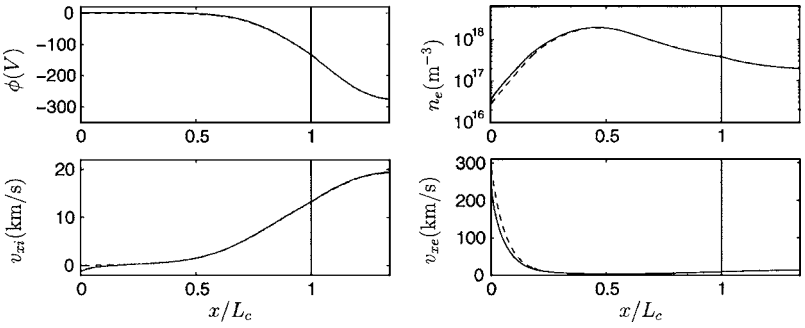

FIG. 6. No-sheath regime. The axial profiles of plasma variables for $-I_{iB}/I_d=5\times10^{-3}$ (solid lines; no-sheath limit) and 0 (solid lines; zero ion backcurrent limit). The vertical line marks the channel exit. The rest of the parameters as in Fig. 2.

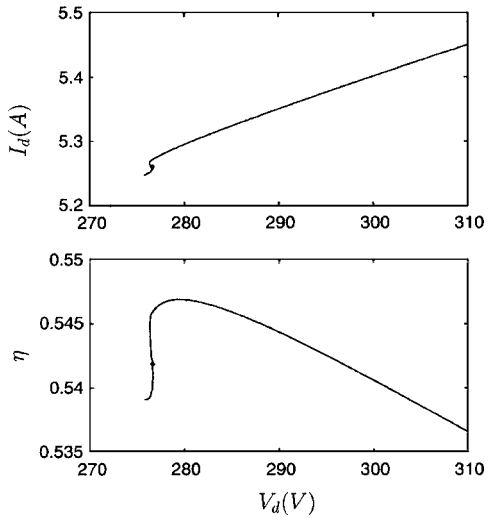

FIG. 7. Current-voltage and efficiency-voltage curves for the case of Fig. 4 ($B_{\max}=230$ G). The dot in the curves corresponds to the regime transition.

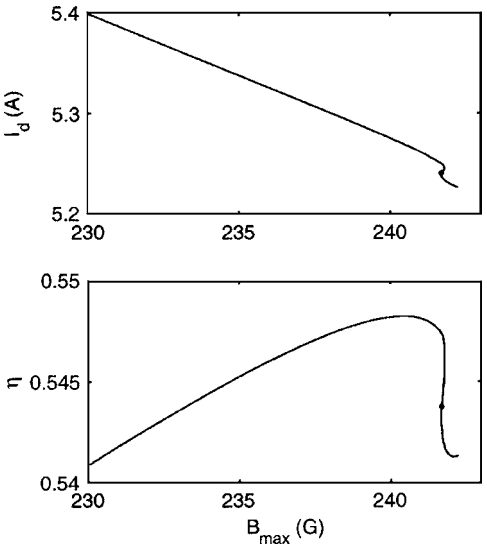

FIG. 8. Discharge current and efficiency vs the magnetic-field strength for $V_d=300$ V. The rest of the parameters as in Fig. 4. The dot in the curves corresponds to the regime transition.

electron velocities. Whereas v_{xeB} increases by one order of magnitude in the parametric interval we are considering, the increment of $v_{\theta e}$ is only 2.5 times. In turns out that inertia bounds the growth of the azimuthal velocity to values of the order of the thermal velocity, independently of the value of the Hall parameter (as long as this is large). For the present case one has

$$m_e v_{\theta eB}^2/2 \sim 3T_{eB}/2, \tag{19}$$

in the no-sheath regime, which implies that energy losses at the anode [Eq. (16)] increase only by a factor of 2 when moving into the no-sheath regime and continue to contribute to the plasma energy losses less than wall deposition and ionization.

The decrease of $T_{e,\max}$ with I_{iB} (i.e., with V_d) implies a reduction of the energy losses at the ceramic walls. This reduction is larger than the increase of the anode losses and thus has a positive effect on the thrust efficiency. The existence of a maximum of η is due to the opposite trends of those energy losses and the voltage efficiency. It is worth noting that the maximum efficiency occurs within the negative-sheath regime, supporting that this regime is the optimal one for thruster operation, as suggested by Zhurin *et al.* and Ahedo *et al.*

Figure 7 plots I_d and η vs V_d for the same cases than Fig. 4; note that the magnetic-field profile and strength are invariant. This figure emphasizes that (i) the operation point of maximum efficiency is within the negative-sheath regime, (ii) the no-sheath regime is very small, and (iii) the current-voltage (C-V) curve is nonmonotonic in that regime. This behavior of the C-V curve and the low plasma density near the anode for the no-sheath regime suggest a possible relation with the fluctuating response and the discharge extinguishment reported for the low-efficiency regime.[1] Furthermore, the change of the curve slope $d\ln I_d/d\ln V_d$, around the no-sheath limit, could be related to the classical knee observed in experimental C-V curves around the transition between the low- and high-efficiency regimes.[16,17]

The transition from negative- to no-sheath regimes can also be achieved by keeping constant the discharge voltage and varying the magnetic-field strength $B_{\max}$. Figure 8 illustrates this case with the curves $I_d(B_{\max})$ and $\eta(B_{\max})$ for $V_d=300$ V. The negative sheath decreases with $B_{\max}$ increasing, and the no-sheath regime corresponds to high values of $B_{\max}$. As in the case of Fig. 7, the maximum of efficiency takes place within the negative-sheath regime and the no-sheath regime leads to a nonmonotonic behavior of $I_d(B_{\max})$. The behavior of that curve suggests again a correspondence with experimental observations, where I_d decreases with $B_{\max}$ until a certain (optimum) value of $B_{\max}$ is reached, and a strong fluctuating response appears.[3]

V. CONCLUSIONS

In order that a macroscopic model analyzes correctly the transition to a discharge without anode sheath, inertial effects on electrons must be considered. For thrusters with the Hall parameter still large at the anode, these effects modify mostly the azimuthal component of the electron velocity in a thin (quasineutral) region around the anode. Electron inertia bounds the azimuthal velocity to values of the order of the electron thermal velocity, which results in the azimuthal to axial velocity ratio to be locally much less than the Hall parameter value.

The negative fall is found to decrease when the discharge voltage decreases (or the magnetic field increases) which seems to agree with experimental observations by Dorf *et al.*, but disagrees with the models proposed by the same research group. In our opinion, this discrepancy is mainly due to the significant variation of the electron temperature profile with the discharge voltage, which they omit. Nevertheless, the reader is referred to Ref. 4, for an alternative discussion of the discrepancy. Also we notice that our model cannot be validated for discharges with negligible magnetic fields in the rear region, as those considered in the

models of Dorf *et al.*; those discharges require to include electron inertia fully in the region where the Hall parameter is small.

As the discharge moves into the no-sheath regime, the ionization region extends towards the anode, thus reducing the voltage efficiency. The electron azimuthal velocity and the temperature profile determine the energy losses at the anode and lateral walls, respectively. The first ones grow moderately, but these are more than compensated by the reduction of the second ones. The different trends of voltage efficiency and energy losses explain the existence of a maximum of $\eta(V_d)$ (for a constant magnetic field), which is situated in the negative-sheath parametric regime.

The *C-V* curves present a slope change and a nonmonotonic behavior around the transition between the two sheath regimes, which could be related to well-known experimental observations, such as the transition to the low-efficiency regime or to highly-oscillatory responses. Nevertheless, the no-sheath regime studied here is too small to extract reliable comparisons with experimental results. These would require to extend the research in two directions: to use a time-dependent model and to extend the study beyond the zero ion backstreaming limit.

ACKNOWLEDGMENTS

This work was sponsored by the Air Force Office of Scientific Research, Air Force Material Command, USAF, under Grant No. FA8655-04-1-3003, and by the Ministerio de Educación y Ciencia of Spain (Project No. ESP2004-03093).

[1] V. Zhurin, H. Kaufman, and R. Robinson, Plasma Sources Sci. Technol. **8**, R1 (1999).
[2] A. Bishaev and V. Kim, Sov. Phys. Tech. Phys. **23**, 1055 (1978).
[3] V. Kim, J. Propul. Power **14**, 736 (1998).
[4] L. Dorf, Y. Raitses, N. Fisch, and V. Semenov, Appl. Phys. Lett. **84**, 1070 (2004).
[5] J. M. Fife, Ph.D. thesis, Massachusetts Institute of Technology, 1998.
[6] E. Ahedo and M. Martínez-Sánchez, in *Proceedings of the 34th Joint Propulsion Conference, Cleveland, OH, 12–15 July 1998* (American Institute of Aeronautics and Astronautics, Washington, DC, 1998) (AIAA Paper No. 98-8788).
[7] E. Ahedo, P. Martínez-Cerezo, and M. Martínez-Sánchez, in *SP-465, Proceedings of the Third Spacecraft Propulsion Conference*, Cannes, France, 10-13 October 2000 (European Space Agency, Noordwijk, The Netherlands, 2000), p. 323.
[8] E. Ahedo, J. Gallardo, and M. Martínez-Sánchez, Phys. Plasmas **9**, 4061 (2002).
[9] E. Ahedo, J. Gallardo, and M. Martínez-Sánchez, Phys. Plasmas **10**, 3397 (2003).
[10] S. Barral, K. Makowski, Z. Peradzynski, N. Gascon, and M. Dudeck, Phys. Plasmas **10**, 4137 (2003).
[11] L. Dorf, V. Semenov, Y. Raitses, and N. Fisch, in *Proceedings of the 38th Joint Propulsion Conference, Indianapolis, IN, 7–10 July 2000* (American Institute of Aeronautics and Astronautics, Washington, DC, 2002) (AIAA Paper No. 2002-4246).
[12] L. Dorf, V. Semenov, and Y. Raitses, Appl. Phys. Lett. **83**, 2551 (2003).
[13] A. Cohen-Zur, A. Fruchtman, J. Ashkenazy, and A. Gany, Phys. Plasmas **9**, 4363 (2002).
[14] Y. Raitses, D. Staack, L. Dorf, and N. Fisch, in *Proceedings of the 39th Joint Propulsion Conference, Huntsville, AI, 20–23 July 2003* (American Institute of Aeronautics and Astronautics, Washington, DC, 2003) (AIAA Paper No. 2003-5153).
[15] E. Ahedo and D. Escobar, J. Appl. Phys. **96**, 983 (2004).
[16] A. Morozov, Y. Esipchuk, G. Tilinin, A. Trofimov, Y. Sharov, and G. Y. Shchepkin, Sov. Phys. Tech. Phys. **17**, 38 (1972).
[17] H. Kaufman, AIAA J. **23**, 78 (1985).